

## **Ovality in Pipe Bends by Finite Element Analysis**

Kaviti. R Vara Prasad<sup>1</sup>, Tippa Bhimasankara Rao<sup>2</sup>

<sup>1</sup>PG Student, Department of Mechanical Engineering, Nimra Institute of Science and Technology

<sup>2</sup>HOD, Department of Mechanical Engineering, Nimra Institute of Science and Technology, Vijayawada, AP, India

---

**Abstract:-** Pipe bends are critical components in piping systems. In the manufacturing process of pipe bends it is difficult to avoid thickening on the inner radius of the pipe bend and thinning on the outer radius of the pipe bend. The cross section of the bend also becomes non circular due to bending process; this tends to cause ovality in pipe bends. The acceptability of pipe bends is based on the induced level of shape imperfections considered. Ovality is the shape imperfection considered for the analysis which varies from 0 to 8%. This study is an attempt to analyze the ovality effect of inlet pigtail bend, INCOLOY 800 ASTM B407 material which is used in hydrogen reformer application. The finite element method is used to model and analyze a stand-alone, long-radius pipe bend with 42.2mm nominal diameter and a 250mm bend radius with specified length. A parametric study was performed in which the bend factor is taken as 1.90 to 2.07. Internal pressure is incremented for each model, until it reaches  $27 \times 10^8$  N/mm<sup>2</sup>. During this process, the bend undergoes plastic instability due to pressure and thermal effect. The results are presented in the form of total deflection and stresses for the incremented internal pressure and the same is computed for various percentage of ovality. The computed results are compared and the effects of total deflection and stresses of the pipe bends are noted.

**Keywords:-** Creep, Ovality.

---

### **I. INTRODUCTION**

Plain pipe bends are commonly used in the piping systems of power plants. Pipe bends are used to convey fluid and to change the direction of the fluid flowing inside. Pipe bends are curved bar with annular cross section whose reaction to external loading is complex. Therefore, the life assessment and failure prediction of pipe bends is an important factor to be considered in the design and safe operation of pipelines. The design life of pipe bends by codes is usually based on the mean diameter formulae for straight pipes, which is applicable to the situations where significant system loads or other external loads are not present.



**Fig.1** Pipes

### **II. BENDING PIPES**

It is subjected to many different kinds of loading load. Sustained load arise from the mechanical force acting on the system under design conditions but for purpose of code design three categories of load type defined: sustained load, occasional load and expansion which include pressure, self-weight, fluid weight and insulation weight. Occasional load also arise from mechanical forces but are expected to occur during only a small proportion of the plant life, such as wind load, seismic load and reaction load due to opening of pressure safety valve. Expansion load arises when the piping system experiences changes in temperature over the operating cycle which causes cyclic thermal expansion of the piping material, inducing thermal stress in the piping components and reaction forces at piping supports and nozzle connected to static equipment.

The bend section may be a potential source of damage during service, particularly in cases where significant ovality and wall thickness variation (thinning/thickening) exist, which are introduced during the

manufacturing process. Hence the acceptability of pipe bends depends on magnitude of the shape irregularities during manufacturing process. In this paper a non-dimensional parameter defining the ratio of internal fluid pressure to allowable stress is computed for tube ratio ranging from 5 to 40 and bend ratio from 1 to 5 to decide the acceptability of pipe bends. In this paper, a specific report from an industry actively engaged in the manufacturing of inlet pigtail pipe bends for hydrogen reformer application has been considered and analysis is done in which the ovality varies from 0 to 8%.

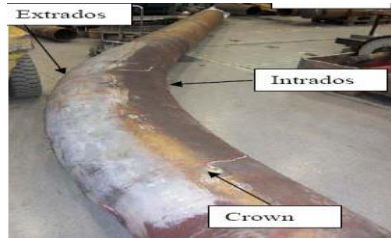


Fig.2 Bend Pipes

### III. DEFINITION OF LOCATION ON BEND

Pipe bends are more flexible than similar length of straight pipe, due to the complex deformation they exhibit under bending loads. When a pipe bend is subjected to a bending load, the cross section of the pipe changes from circle to oval. The deformation of the cross section may enhance or reduce the strength and stiffness of the bend, depending on the direction of the movement. When the bend is pressurized, the behaviour becomes more complex again, due to coupling between the pressure and bending response. When a pressurized pipe bend is subjected to a bending moment, the pressure acts against the ovalization deformation. This paper provides numerical solution of pipe bend subjected to combined pressure and bending with temperature effect based on detailed three-dimensional finite element [FE] analysis. For a wide range of elbow geometry, FE analysis is performed based on elastic-perfectly plastic material INCOLOY 800 ASTM B407 with the small geometry change option. Creep is the progressive time-dependent inelastic deformation under constant load and temperature. Relaxation is the time-dependent decrease of stress under the condition of constant deformation and temperature. For many structural materials, for example steel, both the creep and the relaxation can be observed above a certain critical temperature. The creep process is accompanied by many different slow microstructural rearrangements including dislocation movement, ageing of microstructure and grain-boundary cavitation. The above definitions of creep and relaxation are related to the case of uni-axial homogeneous stress states realized in standard material testing. Under “creep instructors” we understand time-dependent changes of strain and stress states taking place in structural components as a consequence of external loading and temperature. Examples of these changes include progressive deformations, relaxation and redistribution of stresses, local reduction of material strength, etc. Furthermore, the strain and stress states are inhomogeneous and multi-axial in most cases. The scope of “creep modeling for structural analysis” is to develop a tool which allows simulating the time-dependent behaviour in engineering structures up to the critical state of creep rupture. In Chapter 1 we discuss basic features of creep behaviour of materials and structures, present the state of the art within the framework of creep modeling and define the scope of this contribution.

### IV. CREEP PHENOMENA IN STRUCTURAL MATERIALS

The analysis of the material behaviour can be based on different experimental observations, for example, macroscopic and microscopic. The engineering approaches related to the stress-strain analysis of structures and mostly based on the standard mechanical tests. In this section we discuss basic features of the creep behaviour according to recently published results of creep testing under uni-axial and multi-axial stress states.

- **Uni-Axial Creep**

Uni-axial creep tests belong to the basic experiments of the material behaviour evaluation.

A standard cylindrical tension specimen is heated up to the temperature

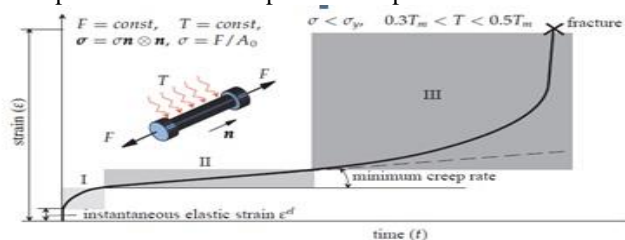


Fig.3 Strain vs time curve under constant load & temperature I. Primary creep, II. Secondary creep, III. Tertiary creep

$0.3 - 0.5Tm$  ( $Tm$  is the melting temperature of the material) and loaded by a tensile force. The value of the normal stress in the specimen  $\sigma$  is usually much less than the yield limit of the material  $\sigma_y$ . The instantaneous material response is therefore elastic. The load and the temperature are kept constant during the test and the axial engineering strain  $\varepsilon$  is plotted versus time. A typical creep curve for a metal is schematically shown in Fig.3. The instantaneous response can be characterized by the strain value  $\varepsilon_{el}$ . The time-dependent response is the slow increase of the strain with a variable rate. Following Andrade [95], three stages can be considered in atypical creep curve: the first stage (primary or reduced creep), the second stage (secondary or stationary creep) and the third stage (tertiary or accelerated creep). During the primary creep stage the creep rate decreases to a certain value (minimum creep rate). The secondary stage is characterized by the approximately constant creep rate.

- **Multi-Axial Creep**

Experimental data obtained from uni-axial tests allow to establish basic features of the creep behaviour and to find relations between strain rate, stress, temperature, time, etc. Most structural members are, however, subjected to multi-axial stress and strain conditions. In order to analyze the influence of the stress state on the time dependent material behaviour, multi-axial creep tests are required. Various techniques have been developed to test materials under multi-axial loading conditions. Examples of multi-axial specimens for creep testing are: thin-walled pipes subjected to axial force and torque, e.g. [168], two- and three-dimensional cruciform specimens subjected to axial forces, e.g. [282, 283], circumferentially notched specimens subjected to axial force, e.g. [146, 251]. Fig.4 shows a thin-walled pipe under the axial force and torque with the magnitudes  $F$  and  $M$ , respectively. Let  $r_m$  be the mean radius of the cross section,  $h$  the wall thickness and  $L$  the gauge length. With the local cylindrical basis  $e_r$ ,  $e_\phi$  and  $k$ , as shown in Fig. 1.7, the stress state can be characterized by the following tensor

$$\sigma = \sigma \mathbf{k} \otimes \mathbf{k} + \tau (\mathbf{e}_\phi \otimes \mathbf{k} + \mathbf{k} \otimes \mathbf{e}_\phi), \quad \sigma = \frac{F}{2\pi r_m h}, \quad \tau = \frac{M}{2\pi r_m^2 h}$$

The deviatoric part of the stress tensor is

$$\mathbf{s} = \sigma (\mathbf{k} \otimes \mathbf{k} - \frac{1}{3} \mathbf{I}) + \tau (\mathbf{e}_\phi \otimes \mathbf{k} + \mathbf{k} \otimes \mathbf{e}_\phi),$$

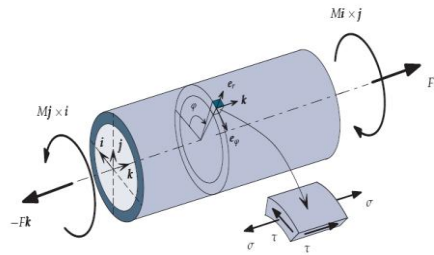


**Fig.4** Thin-walled pipe under the axial force and torque with the magnitudes  $F$  and  $M$

## V. PROBLEM DEFINITION

- **Creep:** It is the tendency of a solid material to move slowly or deform permanently under the influence of stresses.
- **Ovality (Elliptic):** The degree of ovality is determined by the difference between the major and minor diameters divided by the nominal diameter of the pipe.

Percent ovality is

$$C_o = \frac{D_{\max} - D_{\min}}{D} \times 100$$

$$\text{where } D = \frac{D_{\max} + D_{\min}}{2}$$

- **Thinning:** Thinning, which occurs at extrados of the pipe bend, is defined as the ratio of the difference between the nominal thickness and the minimum thickness to the nominal thickness of the pipe bend.

Percent thinning is

$$C_t = \frac{t - t_{\min}}{t} \times 100$$

- **Thickening:** Thickening occurs at intrados and is defined as the difference between the maximum thickness and the nominal thickness divided by the nominal thickness of the pipe bend.

Percent thickening is

$$C_{th} = \frac{t_{max} - t}{t} \times 100$$

The following assumptions are made in the analysis: Linear behaviour, homogeneous isotropic material and steady static state loading. The effects of the following are not considered in the present evaluation: Bourdon’s effect, external pressure, external force, external moments, centrifugal forces due to change of fluid flow direction, effects of friction between the pipe inside fluid and the pipe bend interfaces between the straight pipe before fabricating in to pipe bend and pipe bend surface roughness. The piping system considered a long radius bend with two attached equal length straight pipe runs and the cross section of the bend is assumed to become a perfect ellipse after bending. The mean cross sectional radius of the bend (R) considered as 250 mm, the bend factor incremented from 1.90 to 2.07 and the percentage of ovality varied from 0 to 8. The internal pressure incremented for each model till it reaches 27x108N/mm2.

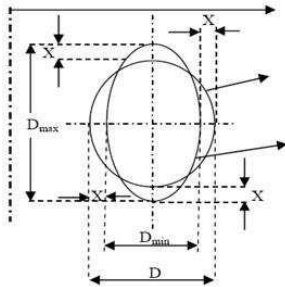


Fig.5 Pipe bend cross section before and after bending runs

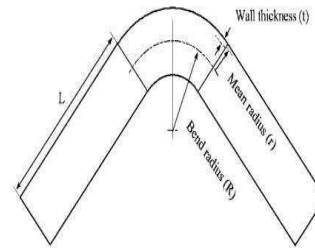


Fig.6 Pipe bends attached to two straight runs

The length of the attached straight piping was chosen to ensure that the bend response was independent for the various percentage of ovality. The major axis of the elliptical shape of pipe bend is assumed to be perpendicular to the plane of bending of the pipe bend. The minor axis of the elliptical shape of pipe bend is assumed to be in the plane of pipe bend. The pipe bend is assumed to be smooth, without ripples and flattening. The pipe bend had a nominal diameter of D=42.2mm and the bend’s axis had a radius of curvature R=250mm to represent a long-radius pipe bend with radius ratio (R/r=11.85). The pipe wall thickness (t) varied between 3.7mm to 3.4mm this corresponds to a variation in the bend factor (h) between 1.90 and 2.07. These values were chosen to represent standard pipe schedules Sch.40S.

Sr.no.	Pipe Parameters	Case 1	Case 2	Case 3	Case 4	Case 5	Case 6
1	Pipe Materials	INCOLOY 800 ASTM B407					
2	Inner diameter $d_{max}$	35.6	36.26	36.6	37.19	38.245	39.3
3	Inner diameter $d_{min}$	35.6	34.14	33.8	32.97	31.915	30.86
4	Inner thickness $t_{max}$	35.6	3.66	3.7	3.916	4.094	4.272
5	Outer thickness $t_{min}$	35.6	3.46	3.4	3.204	3.026	3.2752
6	Outer diameter $D_{max}$	42.2	43.26	43.9	44.31	45.365	46.42
7	Outer diameter $D_{min}$	42.2	41.14	40.5	40.09	39.035	37.98
8	Bend radius	250 mm					
9	Bend angle	90 degrees					
10	Percent of Ovality	0	5	8	10	15	20
11	Working Pressure	27N/mm2					
12	working temp	100 degrees centigrade					
13	Possion's ratio	0.3					

Table.1 Input data

## VI. ANALYSIS PROCEDURE

The piping system configuration has two planes of symmetry and as such can be modelled by a quarter finite element meshes, with appropriate symmetry boundary conditions applied. The pipe bend geometry was modelled in CATIAV5 Wild fire 4 and imported in to ANSYS 11.0 as an IGES file. A convergence study was performed to establish a suitable mesh density for the model. The bend was described by 352670 Nodes and 66060 Elements along the Pipe. The bend is subject to bending and internal pressure loading. The pressure

applied as a surface load along the bend with attached pipe surface. The system assumed to be fixed at both ends, such that the internal pressure gives rise to an axial thrust in the system and the same is applied to the pipe end as an edge pressure, which remains normal to the end of the pipe during deformation. Two loading sequences were considered in the investigation. The internal pressure and temperature were applied to the model simultaneously. The internal pressure was applied to a pre-determined value then held constant of ovality for various percentages.

Temperature–pressure interaction surfaces were constructed by performing analysis of each piping system for different bend geometry.

## VII. RESULTS AND DISCUSSIONS

### ➤ Zero degree Ovality

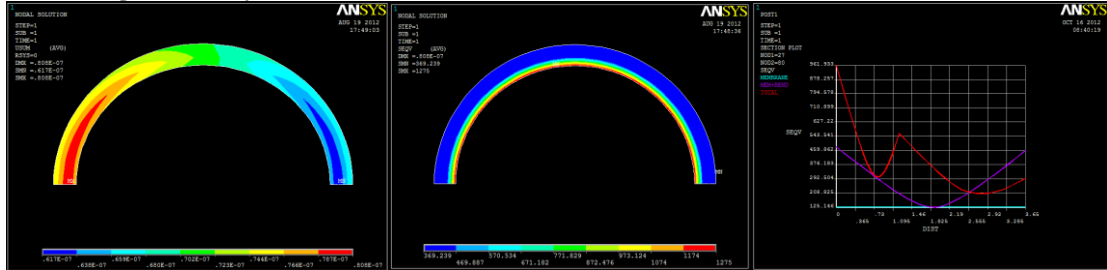


Fig.7 Max Deformation

Fig.8 Von-Mises Stress distribution

Fig.9 SCL Curves

- **Deformation:** Max Deformation is 0.808 mm is obtained at ends and shown below
- **Stress:** Max Von-Mises Stress is obtained 1275 MPA at inner layer of tube.
- **SCL Curves:** Membrane, Mem + Bend & Total Stress, are plotted at Maximum Stress. Total Stress obtained is 961.933MPa

### ➤ Five degrees Ovality

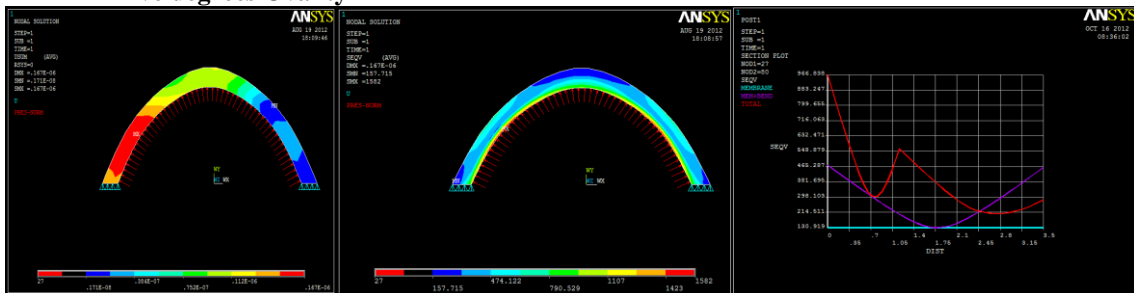


Fig.10 Max Deformation

Fig.11 Von-Mises Stress distribution

Fig.12 SCL Curves

- **Deformation:** Max Deformation is 0.167 mm is obtained at ends and shown below
- **Stress:** Max Von-Mises Stress is obtained 1582 MPA at inner layer of tube.
- **SCL Curves:** Membrane, Mem + Bend & Total Stress, are plotted at Maximum Stress. Total Stress obtained is 966.838 MPa

### ➤ Eight degrees Ovality

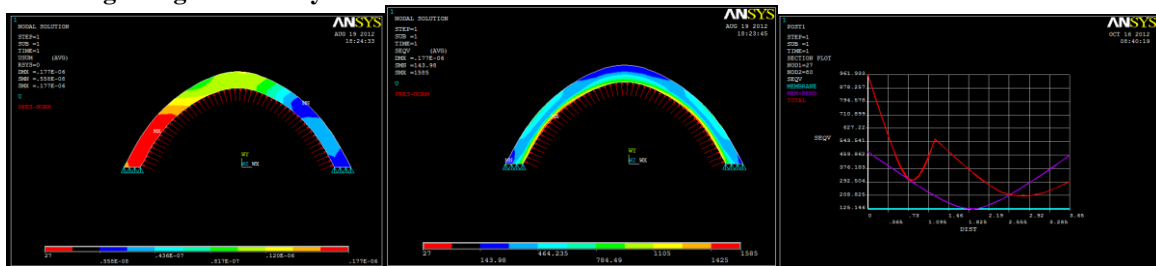


Fig.13 Max Deformation

Fig.14 Von-Mises Stress distribution

Fig.15 SCL Curves

- **Deformation:** Max Deformation is 0.177 mm is obtained at ends and shown below
- **Stress:** Max Von-Mises Stress is obtained 1585 MPA at inner layer of tube.

- **SCL Curves:** Membrane, Mem + Bend & Total Stress, are plotted at Maximum Stress. Total Stress obtained is 961.933 MPA

➤ **10 degrees Ovality**

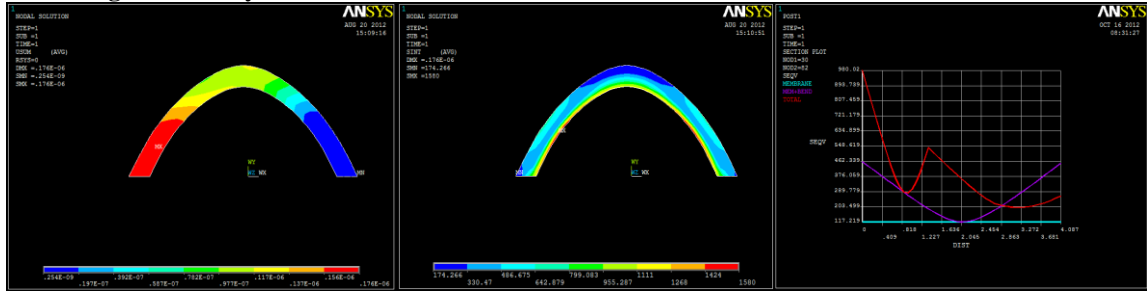


Fig.16 Max Deformation

Fig.17 Von-Misses Stress distribution

Fig.18 SCL Curves

- **Deformation:** Max Deformation is 0.176 mm is obtained at ends and shown below
- **Stress:** Max Von-Misses Stress is obtained 1580 MPa at inner layer of tube.
- **SCL Curves:** Membrane, Mem+Bend & Total Stress, are plotted at Maximum Stress. Total Stress obtained is 980.02 MPA

➤ **15 degrees Ovality**

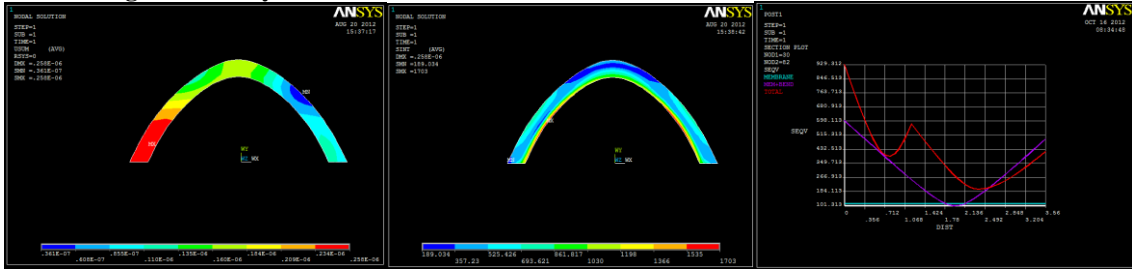


Fig.19 Max Deformation

Fig.20 Von-Misses Stress distribution

Fig.21 SCL Curves

- **Deformation:** Max Deformation is 0.258 mm is obtained at ends and shown below
- **Stress:** Max Von-Misses Stress is obtained 1703 MPa at inner layer of tube.
- **SCL Curves:** Membrane, Mem+Bend & Total Stress, are plotted at Maximum Stress. Total Stress obtained is 929.312MPa.

➤ **20 degrees Ovality**

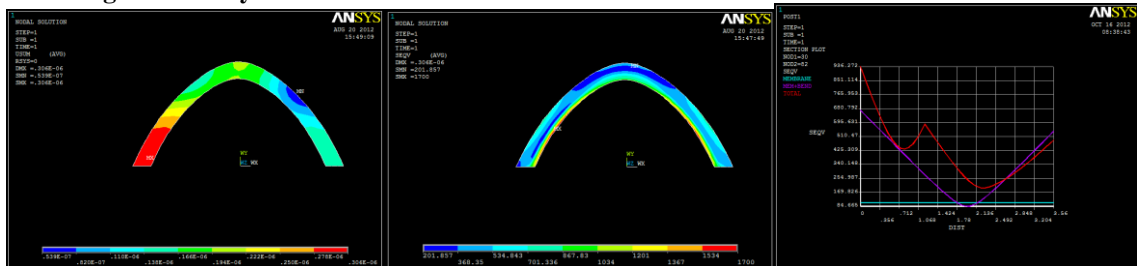


Fig.22 Max Deformation

Fig.23 Von-Misses Stress distribution

Fig.24 SCL Curves

- **Deformation:** Max Deformation is 0.306mm is obtained at ends and shown below
- **Stress:** Max Von-Misses Stress is obtained 1700 MPa at inner layer of tube.
- **SCL Curves:** Membrane, Mem + Bend & Total Stress, are plotted at Maximum Stress. Total Stress obtained is 936.272MPa

$$PM=MEMBRANE, PL+PB=MEMBRANE + BENDING, PL+PB+Q=TOTAL$$

SC L	Case study	Stress Intensity (Mpa)	Allowable Stresses (Mpa)	Descriptions	Result
1	Zero Ovality	112	450	PM(S)	ok
		680	675	PL +PB (1.5 x S)	ok
		937	1350	PL +PB +Q (3xS)	ok
2	5-degree Ovality	130	450	PM(S)	ok
		465	675	PL +PB (1.5 x S)	ok
		966	1350	PL +PB +Q (3xS)	ok
3	8-degrees Ovality	125	450	PM(S)	ok
		470	675	PL +PB (1.5 x S)	ok
		962	1350	PL +PB +Q (3xS)	ok
4	10-degrees Ovality	118	450	PM(S)	ok
		463	675	PL +PB (1.5 x S)	ok
		980	1350	PL +PB +Q (3xS)	ok
5	15-degrees Ovality	110	450	PM(S)	ok
		598	675	PL +PB (1.5 x S)	ok
		930	1350	PL +PB +Q (3xS)	ok
6	20-degrees Ovality	160	450	PM(S)	ok
		500	675	PL +PB (1.5 x S)	ok
		1274	1350	PL +PB +Q (3xS)	ok

**Table.2** Case study of degrees of ovality

### VIII. CONCLUSION

Hence, from the result table it is concluded that the deformation for the ovality change in the pipe is varied like a sine wave form as we can see at zero % ovality the deformation is maximum with a value of 0.808 and then suddenly decreases at 5% ovality and then increases uniformly up to 20% ovality. From the result table it is concluded that the stress at the zero % ovality is 1275 and then it increases up to 1700 for the 20% ovality of the pipe bend.

Therefore, it is concluded that the optimum ovality for the pipe bend is stated as the 5%ovality level.

### REFERENCES

- [1]. Bendick W, Weber H. Utersuchung von Zeitstandsbadigungund Erschopfung an eiem Rohrbogenaus 14MoV 6 3 VGB Kraftwerkstechnik September 1989; 69(9):936-944.
- [2]. Hyde TH, Sun W, Williams JA. Prediction of creep failure life of internally pressurised thick walled Cr MoV pipes. Int J Pres Ves Piping2000; 76:925–33.
- [3]. Hyde TH, Yaghi A, Becker AA, Earl PG. Comparison of toroidal pipes and 908 pipe bends during steady-state creep. Proceedings of the fifth international colloquium on ageing of materials and methods for the assessment of lifetimes of engineering plant, Cape Town; April1999. p. 305–17.
- [4]. Hyde TH, Sun W, Williams JA. Life estimation of pressurised pipe bends using steady state creep reference rupture stresses. Int J Pres Ves Piping 2002; 79:799–805.
- [5]. Hyde TH, Sun W, Becker AA. Effect of geometry change on the creep failure life of a thick-walled Cr MoV pipe with a circumferential element. Int J Pres Ves Piping 2004; 81:363–71.
- [6]. Hayhurst DR. The role of creep damage in structural mechanics. In: Wilshire B, Owen DR, editors. Engineering Approach to High Temperature. Swansea: Pine ridge Press; 1983. p. 85–176.
- [7]. Hyde TH, Becker AA, Sun W. Validation of FE approaches for modelling creep continuum damage mechanics. Proceedings of the seventh international conference on computational structures technology .Lisbon; September 2004.